A Modeling Approach to Predict Fretting Fatigue on Highly Loaded Blade Roots

Patrick Wackers
Victor Arrieta

MTU Aero Engines GmbH,
Munich,
Bavaria 80995, Germany

Marcel Alquezar-Getan
ATENA Engineering,
Munich,
Bavaria 80995, Germany

Andrei Constantinescu
Habibou Maitournam

LMS-CNRS,
École Polytechnique Palaiseau,
Palaiseau Cedex 91128, France

A lifing technique for predicting fretting fatigue on highly loaded blade-disk attachments has been developed and calibrated. The approach combines extensive testing on nickel and titanium based alloys using a specially devised multiaxial fretting test machine and an analytical lifing procedure, based on finite element contact calculations and multiaxial shakedown fatigue models. In order to reproduce realistic operational conditions and standardize testing conditions, a special fretting fatigue testing machine with high temperature testing capabilities was developed. The machine was employed to perform systematic testing under prescribed load and displacement conditions at representative temperatures. Making use of FEA, the rig test results were calculated to identify relevant parameters such as friction coefficient, slip conditions, and machine compliance. The computation procedure involves the calculation of several major loading cycles until a stabilized response of the structure is achieved. The material response is assumed to be elastoplastic, and a nonlinear friction law (space and time) was applied. From the computed mechanical variables, several life prediction models are benchmarked to establish their capabilities to predict fretting fatigue life. Finally, a most promising life estimation procedure was applied to predict life in a real compressor blade-disk attachment. Predicted failure location and number of cycles to failure are compared against engine test results. The experimental-analytical approach has the potential to predict fretting fatigue risk during the design phase on highly loaded joints, as well as estimating the preventive overhaul intervals for parts already in service. [DOI: 10.1115/1.3205026]

1 Introduction

Aeroengines incorporate a large number of mechanical joints, for which fretting fatigue and wear are important life controlling factors. All mechanical components will suffer from degradation, and eventually, fatigue or wear out along their operational lifespan. Therefore, fretting fatigue and wear control need to be considered as a design criterion, even if they may be subsequently dismissed or controlled by design experience and/or overhaul. Whereas wear is associated with long term operation, fretting fatigue is associated with short term failures (reduced numbers of cycles compared with plain fatigue). Despite comparable economical impact, safety requirements on aeronautic components make the prediction and avoidance of fretting fatigue a critical reliability issue, and so it is the focus of current efforts.

Gas turbines and aeroengines, in particular, are known to suffer from fretting fatigue on components that undergo repeated small relative displacements under high compressive forces, for example, blade-disk attachments, splined shafts, and to a lesser degree of bolted flanges.

A classical case are dovetail or fir tree shaped blade-disk connections (see Fig. 1). They have to endure high centrifugal forces leading to elevated contact and bulk stresses, which, combined with relative small displacements that occur as the engine undergoes its operational cycle, make fretting fatigue an important, if not the main design criterion. The possibility of blade root failure with its operational consequences infers that any life improvement or at least reliable life prediction has an important bearing on the integrity and overall cost of the engine.

Along the years, aeroengine manufacturers and users have collected experiences on how to control fretting fatigue and wear. As in conventional fatigue, simple design rules are helpful to avoid fretting fatigue in most situations [1], but do not provide a quantifiable life estimation, and therefore, do not support design optimization efforts to optimize weight and durability.

Many palliative methods have been devised showing a wide variety of effectiveness. They help to overcome critical situations but do not provide a reliable method to predict and control fretting fatigue and wear. Despite of research efforts in the last 50 years [2], where the main controlling mechanisms of fretting fatigue and wear have been identified, a consistent, reliable, and industrially applicable life model continues to be a challenge.

The purpose of the present paper is to present a life estimation method for fretting fatigue, based on (i) a mechanical analysis of the complete problem, and (ii) a fatigue criterion based on classical mechanical variables. It will be shown that the method is capable of predicting and quantifying both the failure location and cycle number to crack initiation for fretting fatigue rig test results, as well as for an aeroengine application. Several aspects will be discussed: the importance of the friction law on mechanical variable determination, comparison of different fatigue criteria, and consideration of stress gradient effects.

1.1 Fundamental Aspects of Fretting Fatigue. Fretting fatigue occurs when two bodies pressed together undergo a small localized relative displacement, typically of the order of 10–30 μm. It differs from normal wear such that the displacements are much smaller, and that any wear debris remains trapped between the two surfaces in contact. Under the contact conditions previously described, a mixed stick-slip regime is established between the bodies. It is well known that fretting fatigue cracks will develop in the transition zone between stick and slip regions [3].

Crack initiation under fretting fatigue condition depends mainly on the contact stresses, and occurs in the vicinity of the highly localized stress concentrations caused by the frictional forces between the surfaces in contact. Crack propagation, on the other hand, responds to the bulk stress field away from the surface.

Fretting fatigue damage is also observed to be a function of slip amplitude and bulk stress. Whenever the slip amplitude is big

Manuscript received April 8, 2009; final manuscript received April 15, 2009; published online May 10, 2010. Review conducted by Dilip R. Ballal.

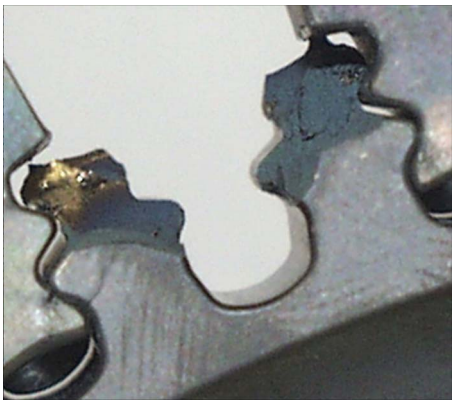

Fig. 1 Fretting-fatigue damage on blade-disk attachment

enough, the mechanism of fretting gives way to conventional wear. The net effect is that fretting fatigue strength decreases with an increasing slip (starting from zero) until a point is reached where abrasive wear governs the process and the strength increases again.

It is generally recognized that the fretting fatigue process can be divided into three distinct phases: (i) crack initiation, (ii) short crack propagation, and (iii) long crack propagation.

Due to safety issues, most aeronautic components should be designed in such a way that they can fulfill their life targets before a crack is initiated, i.e., estimating the number of cycles until an engineering crack size is reached. Therefore, the present work is tailored to predict crack initiation life. Real sizes of engineering cracks are material and structure dependent, and will not be discussed here due to confidentiality issues.

There is an inevitable dependence on local conditions at the contact interface, and it may be necessary to consider variables such as material microstructure and asperities. Studies on these effects were already done by Hofman et al. [4]. However, in the present study, such variables will be considered part of the friction coefficient, and therefore, will not be addressed.

During the last 50 years, intense research efforts have been devoted to find out the controlling parameters on fretting fatigue. A number of attempts have been made to apply global stress or displacement based parameters to the prediction of initiation life. Ruiz et al. [5] proposed a criterion, based on the density of dissipated energy multiplied by the direct stress component parallel to the surface. Hills et al. [6] tested similar parameters on different geometries with good results. However, the Ruiz parameter is totally empirical, and deriving design lines from it is a difficult task.

More recently, stress based criteria using multiaxial fatigue initiation parameters were proposed. Szolwinski and Farris [7] have combined the Smith–Watson–Topper approach with the critical plane concept to successfully predict fretting fatigue experiments, assuming an analytically derived stress field. Neu et al. [8] have presented a concept to predict fretting fatigue, based on fracture mechanics and equivalent crack size to characterize crack initiation. A global approach was employed by Fouvry et al. [9] who have combined a volume averaging method with the Dang Van criterion [10,11], and have shown that this can give more realistic life predictions for cases where the stress field varies very rapidly.

The above mentioned Dang Van model combined with representative volume averaging (REV) meets the needs stated on paragraph 1.2, and therefore, it is the selected model for a first application to an aeroengine fretting fatigue problem.

Nevertheless, the Dang Van model is purely based on stresses, and from a mechanical point of view, its application is not valid for cases in which the structure's shakedown state is plastic.

This methodology has already been successfully applied in a series of industrial applications. A general review is given in Ref. [12]. An application to rolling contact in Ref. [13] and an application to fretting fatigue experiments in Refs. [14–16] shall also be highlighted in this context.

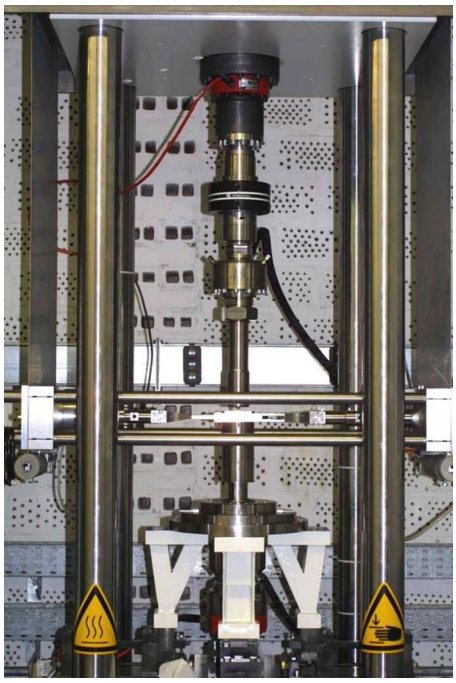

Fig. 2 View of the multiaxial fretting rig

In order to apply the criterion on a structure, different steps have to be performed.

- The first step is a complete elastoplastic analysis under cyclic loading. The result should asses that the structure is macroscopically under an elastic shakedown state in all its points. If a plastic shakedown state occurs in a series of points, a low cycle failure should be expected, and criteria related to the dissipated energy or the inelastic strain should be applied. For a general overview of the passage between the high cycle and the low cycle fatigue domains, see Ref. [17].
- The second step is the fatigue analysis, in which the fatigue criterion is checked in all points of the structure.

2 Experiments

An extensive test series has been performed for both Inconel 718 (IN718) and Titanium 64 (Ti64) in self-contact.

Two types of experiments have been used: (i) push-pull experiments to establish the fundamental fatigue parameters, and (ii) fretting fatigue experiments to test the material under the relevant loading conditions.

The fretting fatigue experiments were performed on a new testing rig that was developed especially for the presented work. A view of the fretting rig and cross section of pads and specimen are shown in Figs. 2 and 3, respectively.

The contact geometry used, as depicted in Fig. 4, was the well established flat with rounded edges on a flat configuration. The basis of the rig is formed by a hydrodynamic low cycle fatigue (LCF) pulser that applies a cyclic fatigue load $\sigma_f(t)$ with an R-ratio of 0.01 to a fatigue specimen with a rectangular cross section of 60 mm^2. The novelty is a transversal loading frame, suspended from the top of the machine by two large flexible sheet metal plates that ensure a symmetric application of the normal load to the specimen.

The transversal loading is applied by a hydraulic actuator that presses two pads against the axial specimen from the side, ap-

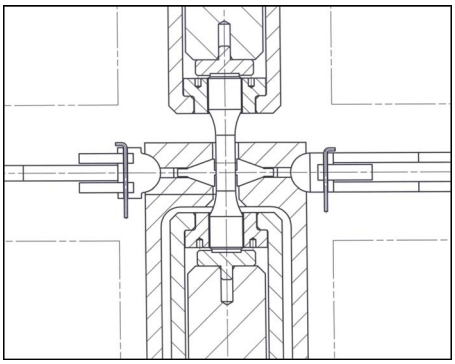

Fig. 3 Cross section of pads and specimen

proximately centered on the specimen gage length. The pads have been manufactured by precision grinding to a total axial length of 2.5 mm, with a flat section of 2.1 mm and two 0.2 mm radii at the edges (see Fig. 4).

A crucial difference from existing rigs is that the pads are additionally guided by a support frame that is suspended by four bending beams from the bottom of the main frame. These beams are adjustable in length, allowing to influence the rig stiffness, and thus, the slip state between pads and specimen for fixed axial and normal loads. By increasing the support stiffness, the pads will experience more resistance trying to follow the specimen elongation, and the contact characteristic will change from partial to full slip.

Generally, the test setup is capable of applying loads of up to 100 kN in the longitudinal direction, and 25 kN in the transversal direction. Additionally, the setup can be heated with an electric furnace up to temperatures of 800°C.

Load cells located above and below the contact in the main load train allow estimation of a mean friction coefficient over the complete contact area during cycling. It is well understood that this is only possible as long as the contact is in a full slip state, which is usually only the case during the very first cycles of an experiment before a stabilization in the partial slip regime is reached. As soon as the contact reaches a macroscopic stick state (either full stick or partial slip), the friction coefficient cannot be measured reliably.

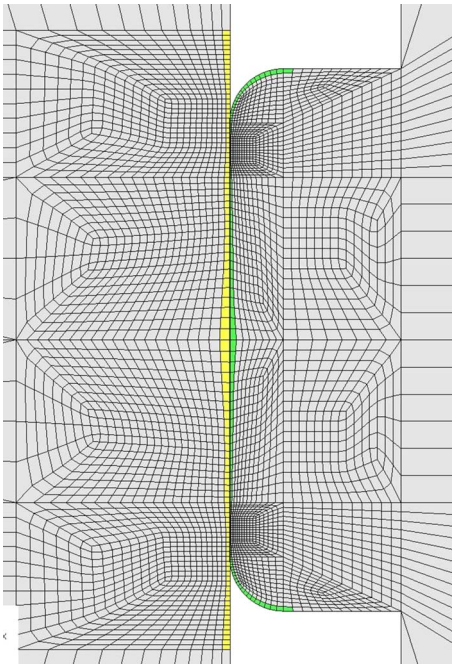

Fig. 4 Finite element mesh at rig contact zone

Therefore, the test sequence is designed to monitor the elongation of the main specimen, and as soon as the measured elongation diverts by more than 10% from the stabilized value at the beginning of the test, the specimen is considered to be cracked, and a gradual reduction of the transversal load, i.e., the contact pressure, is initiated. Consequently, the contact turns back into full slip at the very end of the test, just before the specimen breaks. Therefore, the presented setup enables the user to retrieve both the initial friction coefficient μ_i, as well as the final or stabilized friction coefficient μ_s from each fretting fatigue experiment. This information will later be used to set up a nonlinear friction law (see Sec. 4.1).

In all experiments, cracks nucleated at the periphery of the full stick region and coalesce to form a propagating crack. There were a few experiments on which cracks have nucleated but not propagated. They were characterized by high contact pressure and low axial load. As expected, when the stress field is not strong enough to propagate short cracks, component failure does not take place. These experiments were not included in the database because it was not possible to determine the point where cracks appeared without disturbing (stopping) the experiment.

3 Mechanical Analysis

The mechanical analysis is based on a 2D finite element model using a commercial FEA solver (ABAQUS). The temperature dependent constitutive law of the materials is considered as elastoplastic, with a nonlinear combined isotropic and kinematic work hardening of the Armstrong–Frederick type. Special emphasis was put on the definition of the friction model as described in Sec. 3.1.

A typical mesh at the contact zone is shown in Fig. 4. Four node linear plane strain elements were used for the analysis (CPE4I). Mesh density was chosen to be approximately 10 μm (average element edge length) in the region where the highest stress gradients are expected (transition region between the flat part and the rounded edge of the pad).

Symmetry conditions were used, so that only half of the specimen and only one contact pad are modeled. Test rig compliance is taken into account by spring elements with variable stiffness. The support spring stiffness is varied in accordance with the value used for the corresponding test.

3.1 Friction Model. The friction model used for the FEA was derived from frictional measurements conducted on the biaxial fretting rig presented in Sec. 3. For room temperature tests, usually, some initial slip was experienced, which was useful to determine the initial friction coefficient μ_i. For higher temperatures, special incremental slip tests had to be performed to identify the initial value, since no initial slip would occur under normal testing conditions, see Ref. [6]. The stabilized value μ_s was usually identified by a gradual reduction of contact pressure at the end of the test, which forces the contact back into full slip during cyclic bulk stress loading. This so called "downslope" sequence was initiated once a crack was suspected in the specimen, which was decided by monitoring the specimen elongation along the test. This elongation will sharply increase once a crack of sufficient size has been initiated.

The model adopted to link both the initial and the stabilized friction coefficient is a simplified version of the law that was first published by Cheikh et al. [18]

$$\mu = \mu_i + \mu_s(1 - e^{-k\delta}) \tag{1}$$

The evolution law is based on the friction coefficient dependency on the accumulated relative slip at each node in contact, e.g., at each node, the relative displacement with the opposite body is summed up along the cycle and for each computed cycle. As a result, a friction law as a function of space and time is defined.

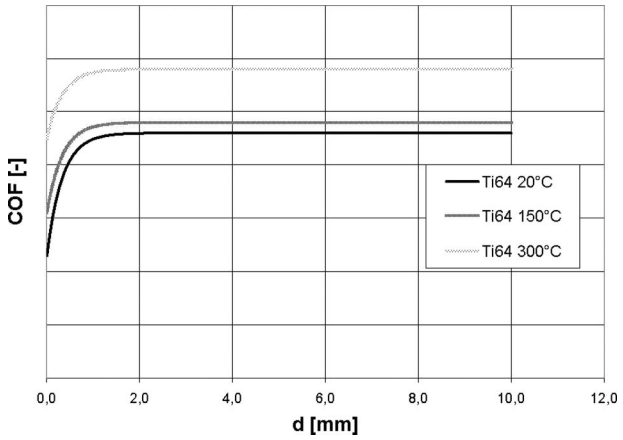

Fig. 5 Friction coefficient evolution for Ti64 at different temperatures with $k=3$

After initial contact at $\delta=0$, the friction coefficient will increase from μ_i, based on the accumulated relative slip at each node.

The parameter k determines how fast the transition from the initial value to the final value will evolve. Since in the test, this evolution takes several thousands of cycles, it would be computationally too expensive to define k, based on test data.

It is proposed within this work to use k as an acceleration parameter to simulate the μ evolution in a shorter number of cycles. Practical values of k have been found to range between 0.2 and 3.0.

It is well understood that this model is only capable of simulating contacts in partial slip or full slip with small sliding distances (smaller than 10% of the total contact length).

In any gross slip situation, i.e., a wear situation, other mechanisms will become predominant, and the presented model will not yield reasonable results.

Figure 5 shows the friction coefficient evolution for a Ti64-Ti64 pairing for different temperatures and $k=3$. Figure 6 shows the stabilized friction coefficient distribution along the contact interface for a IN718-IN718 pairing at 650°C, obtained with the presented friction law. A summary of the range of test parameters used for each material pairing is shown in Table 1.

From the figure, it is obvious that the friction coefficient experiences a strong evolution in the partial slip zone only (left part of the figure), whereas it remains almost constant in the stick zone (right part of the figure).

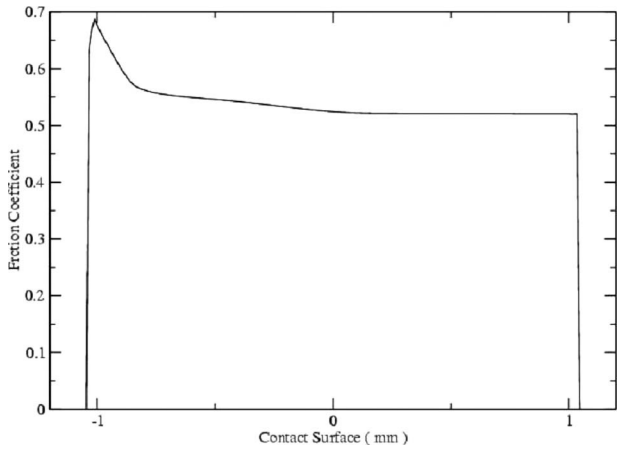

Fig. 6 Friction coefficient distribution along the contact interface for IN718 at 650°C, derived from a 2D FEA

4 Fatigue Analysis

The fatigue analysis is based on the application of a fatigue criterion on the computed mechanically stabilized stress-strain cycles. The encountered stabilized cycles were elastic or plastic shakedown or ratcheting, but only loops corresponding to a shakedown state can by analyzed by the criteria.

We shall now distinguish between stress based models applied for the high cycle fatigue regime when elastic shakedown occurs and strain based models that are applicable for the low cycle fatigue regime when plastic shakedown occurred.

The results discussed in this presentation will only focus on the stress based life prediction models. The tested high cycle fatigue criteria under investigation were Sines [11,19,20], Crossland, and the Dang Van criterion [10,21,22].

After a thorough comparison of predictive capabilities of the models mentioned above, the Dang Van criterion was chosen for an in-depth investigation, and thus, the presented results were produced with the Dang Van model.

The Dang Van model is based on a two-scale approach, passing the macroscopic load at the grain level, and assuming that for an infinite lifetime, elastic shakedown should occur at both the macroscopic and the mesoscopic scales.

It is expressed as an inequality, relating the mesoscopic shear and hydrostatic stress on slip planes at all instants of the cycle so that damage loading can be precisely characterized. The usual form of the criterion is

$$\mathrm{Max}\_(t,n)\,\tau(t) + a\sigma_H(t) < b \tag{2}$$

where $\sigma(t)$ and $\sigma_H(t)$ are the instantaneous mesoscopic shear stress and hydrostatic stress, respectively, and a and b are the material constants to be determined by two different classical fatigue tests (for example, reversed traction and torsion). The Papadopoulos criterion will replace the maximal resolved shear over all normals with the smallest radius of a hypersphere encompassing the mesoscopic stress path. Both criteria give similar results in terms of lifetime predictions, but the Papadopoulos criterion is faster to compute numerically.

If the inequality is satisfied for both criteria, the corresponding material volume is subject to an infinite lifetime under the prescribed loading. If not, a crack will initiate, and the structure will fail after a number of cycles, which is proportional to the extent by which the criterion was overrun.

In the present work, we have extended the Dang Van criterion from the prediction of the infinite lifetime to the finite lifetime domain. This has been obtained by assuming that the material coefficients are determined for a given lifetime so that actually $a=a(N)$ and $b=b(N)$. In order to extract the value of the respective contact, we have used a logarithmical interpolation technique, based on the Woehler curve, which is the characteristic of the material in question that interpolates between the life lines defined for a constant number of cycles in p, τ-space (see Fig. 7).

Table 1 Summary of the range of test parameters used for each material pairing

Material	$T_{\min}$ (°C)	$T_{\max}$ (°C)	$\sigma_{f,\min}$ (MPa)	$\sigma_{f,\max}$ (MPa)	$p_{\min}$ (MPa)	$p_{\max}$ (MPa)
Ti64	20	350	200	600	300	500
IN718	20	650	400	750	300	750

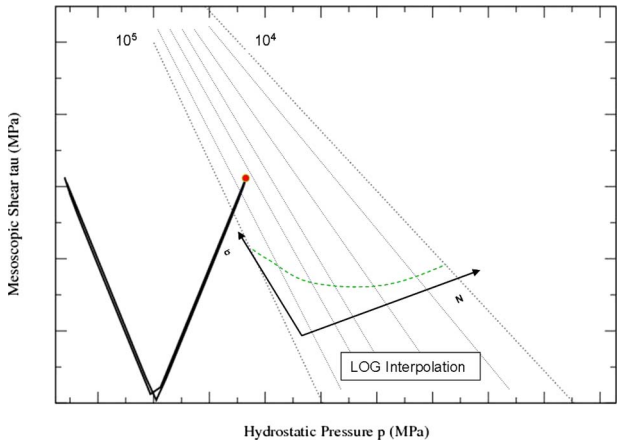

Fig. 7 Interpolation technique for Dang Van

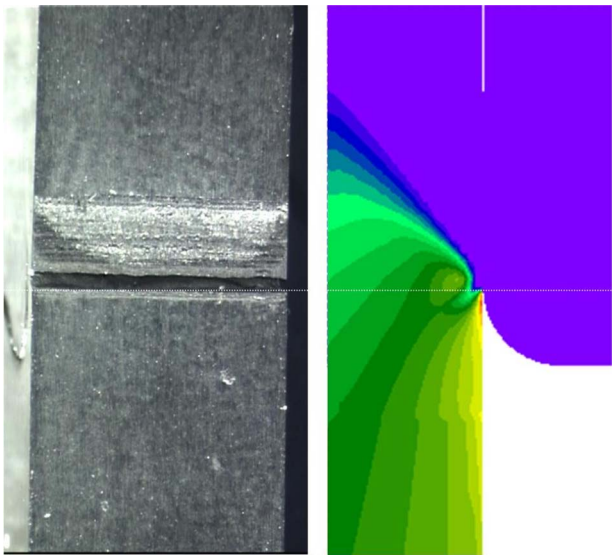

Fig. 8 Failure location in test compared with FEA damage distribution

The constants a and b of the Dang Van criterion can be obtained from uniaxial fatigue data using two fatigue data sets tested at different R-ratios

$$a = \frac{3}{4}\left(\frac{f_{R1} - f_{R2}}{\frac{f_{R1}}{1-R_1} - \frac{f_{R2}}{1-R2}}\right) \tag{3}$$

$$b = \frac{f_{R2}}{2} + \frac{f_{R2}}{2(1-R_2)}\left[\frac{f_{R2} - f_{R1}}{\frac{f_{R1}}{1-R_1} - \frac{f_{R2}}{1-R_2}}\right] \tag{4}$$

where R_1, R_2 and f_{R1}, f_{R2} are the corresponding R-ratios and fatigue limits for the two data sets.

4.1 Lifetime Prediction Results. The method presented in Sec. 5.2 has been applied to the experimental results from the fretting fatigue rig.

As the life prediction model is intended for crack initiation, and the experimental results represent full life, crack initiation and propagation is necessary to differentiate the number of cycles corresponding to each domain. For some experiments, a load drop was observed once a crack has reached an engineering size, therefore allowing regime differentiation. Whenever a load drop was not evident, a linear elastic crack propagation calculation, assuming an engineering crack size as initiation, was performed to estimate the crack propagation life. Finally, crack propagation cycles are subtracted from the total component life to estimate the crack initiation life.

By looking at Fig. 8, it is possible to note that spatial localization of the critical point, according to the Dang Van (DV) criterion, corresponded precisely with the points of crack initiation, which is at the end of the full stick region at the lower contact edge.

However, the predicted lifetime showed a conservative tendency, i.e., the estimated life was much lower than the one obtained from the fretting tests. This could have been expected as the stress and strain gradients are very high at the end of the pad, and it is well known that a high stress gradient will affect the prediction as it is in the case with notched specimens [23]. In order to eliminate this effect, an averaging technique was established, which is explained in detail in Sec. 5.4.

4.2 Stress Gradients Effects—REV. There are three well known techniques to correct fatigue predictions with respect to notch or stress gradient effects: (a) averaging of stresses in a representative volume, (b) computing the lifetime from stresses computed at a distance from the critical spot, and (c) amending the fatigue prediction.

The procedure proposed here is a variant of the averaging of the fatigue criterion, and falls into category (c). It collects all nodal mesoscopic Dang Van loading paths (τ, σ_H) in a certain representative element volume (REV), and averages the loading paths of all the nodes in the volume for each time instant. The averaging was conducted over a cube with a length scale of 80 μm, which is large with respect to the 5 μm size of the microstructure, but correlates well with the scale taken into account in literature for similar problems [9]. The 80 μm representative element volume edge length was determined by applying the Dang Van criterion to fatigue data of uniaxially loaded notched specimens with different notch factors (K_t=2.1 to 4.0). It was observed that evaluating the Dang Van criterion at the most critical location would only yield too conservative life prediction results. The representative volume element was then adjusted until the best match between the tested lifetime and prediction was achieved for both notch factors.

The averaging procedure was implemented directly in an open source postprocessing tool [24].

The difference in the prediction, with and without applying the representative volume element technique, can be seen in Fig. 9 for the mesoscopic loading path, and in Figs. 10 and 11 in comparison of predicted and experimental lifetimes for IN718 at room temperature. The figures show that the postprocessing with a REV

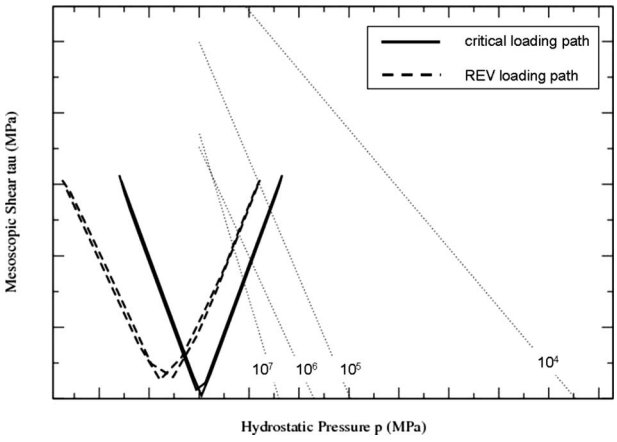

Fig. 9 Representative volume technique in a Dang Van diagram—critical and averaged loading paths

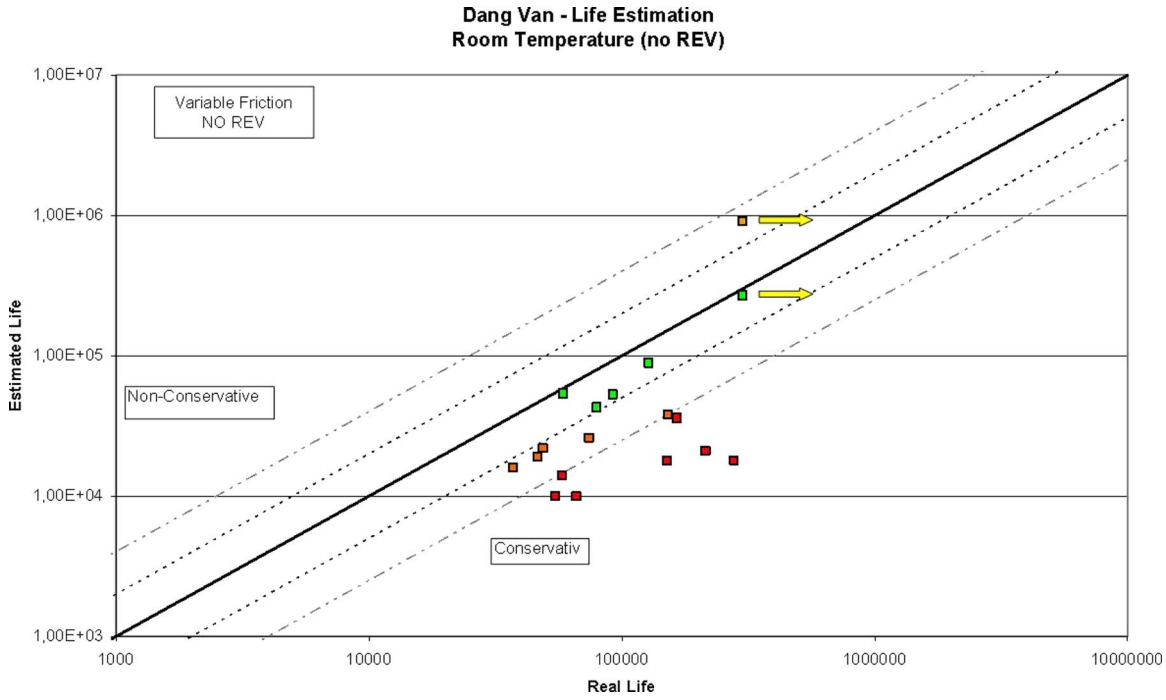

Fig. 10 Dang Van real versus estimated life plots of Inconel—20°C without REV

yields less conservative results than the results without a REV.

By looking at the mismatch of the prediction in a logscale on a histogram, it can be noted that by employing the REV, the distribution of the prediction changes from a rather broad curve on the conservative side to a rather well centered normal distribution (see Figs. 12 and 13 for comparison). The standard deviation is reduced from 0.32 without a REV to 0.25 by employing the REV technique.

Let us now consider the physical background for this procedure. Previous studies have shown that for notched specimens where high stress gradients govern the fatigue behavior in the notch root, the REV technique also improves the prediction [23].

A similar effect can be seen with fretting experiments as high stress gradients are present at the edges of contact due to the contact geometry chosen (flat with rounded edges).

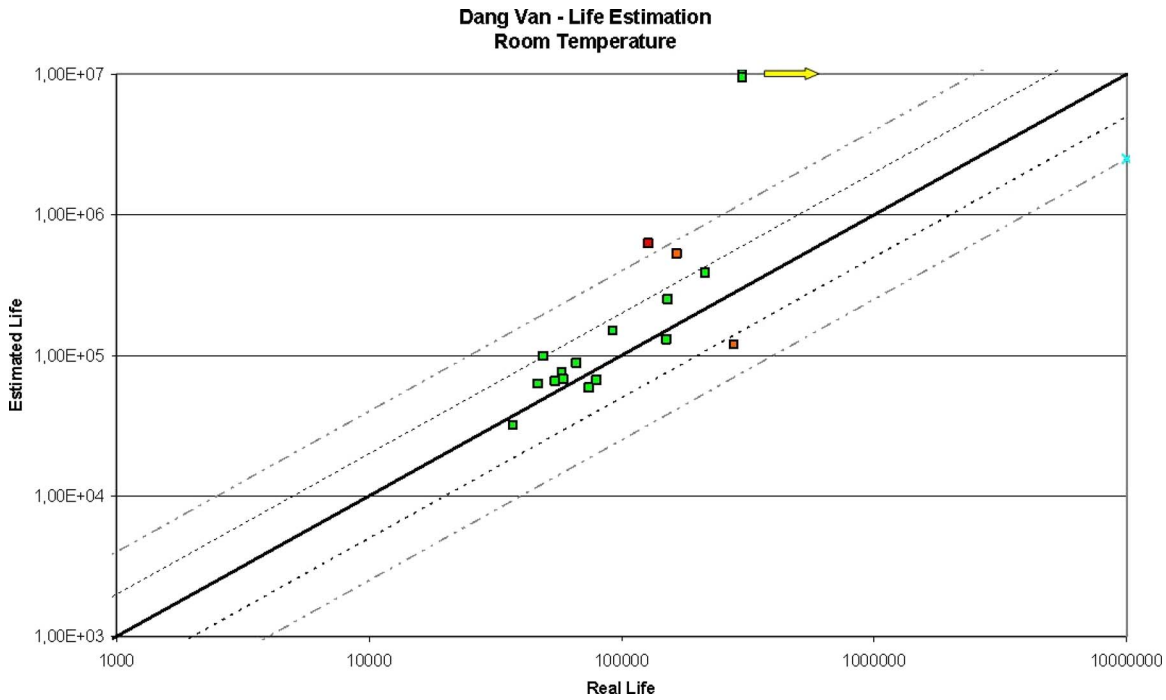

Fig. 11 Dang Van real versus estimated life plots of Inconel—20°C with REV

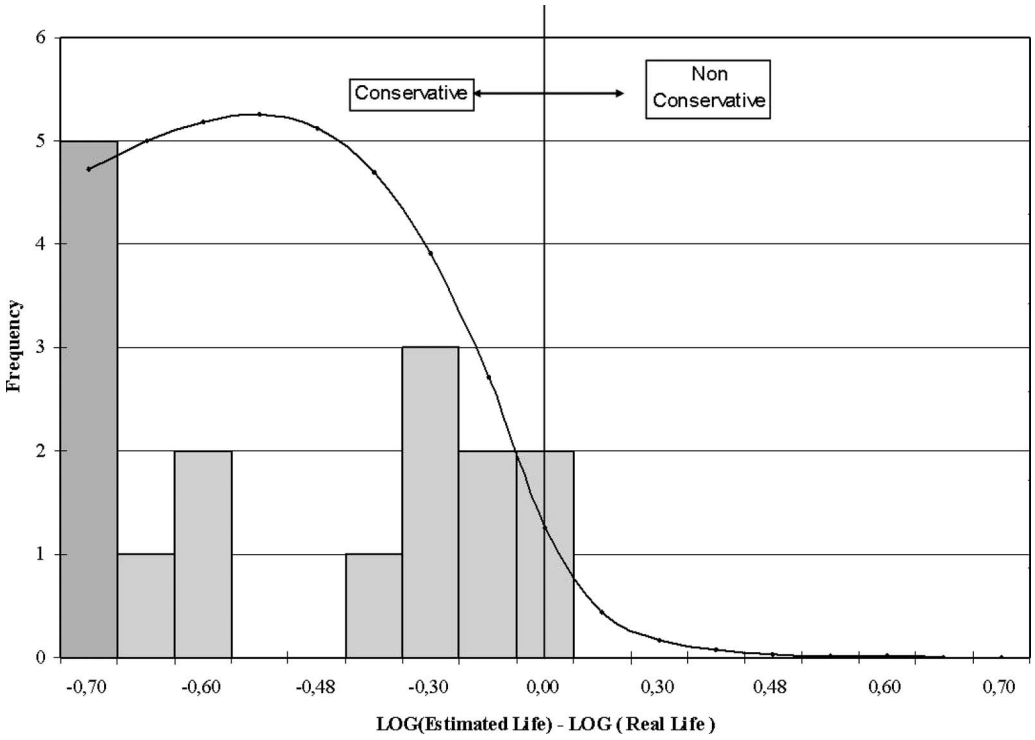

Fig. 12 Histogram of the Dang Van prediction for IN718 at room temperature without REV

Averaging the DV criticality in a volume, comparable to the material grain size, basically determines the grain criticality, which is thus the determining factor for initiating a crack.

5 Engine Test Case

To verify the developed lifing criterion on a real application, an engine test case was selected. The example is a high pressure compressor blade presented in Fig. 14.

The blade under investigation showed early cracking due to fretting fatigue in the titanium blade root during development test runs after less than 4000 cycles. In later development stages, coatings were developed to overcome this shortfall but we will use this example to test the accuracy of our lifing procedure.

One blade and the corresponding disk segment are modeled with TET10 Elements (Blade) and HEX20-Elements (disk) in ABAQUS (see Fig. 14). Centrifugal and gas loads are applied on the structure to simulate the correct loading state of the blade and contact surfaces.

Twenty loading cycles from zero to the redline speed are simulated until a stabilized material response is obtained. Furthermore, both the combined hardening models, as well as the variable friction law (see Sec. 4.1), have been employed for this simulation.

As the structure stabilizes in an elastic shakedown state, the fatigue estimation technique presented in Sec. 5.4 is employed to estimate the failure location, and predict the number of cycles to failure.

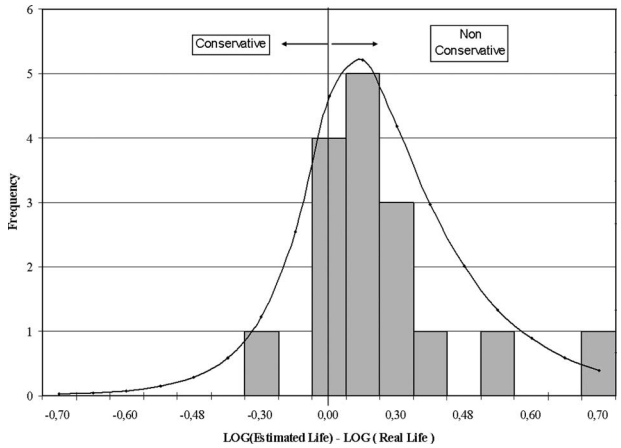

Fig. 13 Histogram of the Dang Van prediction for IN718 at room temperature with REV

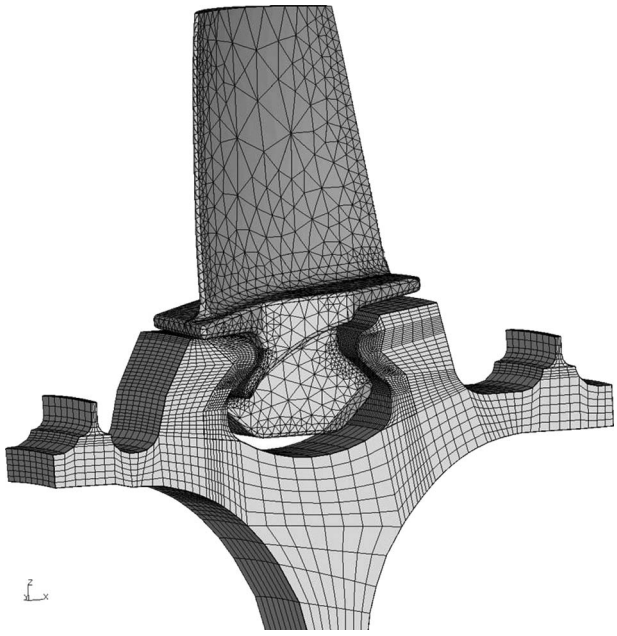

Fig. 14 3D FE mesh on blade root

Fig. 15 Friction coefficient distribution on blade contact surfaces

In Fig. 15 a graphical representation of the friction coefficient on the pressure and suction side of the blade root is given. It can be clearly seen that the friction distribution reaches different mean values on the two sides, and does not evolve evenly along the circumferential length of the contact surface.

The failure location found as a result of the FEA analysis with subsequent Dang Van life prediction corresponds very well with the damage location observed during development test runs. A direct comparison is shown in Fig. 16, where the white lines on the left picture indicate the locations where cracks could be detected after inspection on development test runs.

Figure 17 shows the corresponding critical Dang Van REV loading path for the most critical location.

From Fig. 17, it is obvious that the critical loading path is exceeding the 10^4 constant life line by far. No interpolation is possible for this case since a 10^3 constant life cannot be established in the Dang Van diagram due to large plastic deformations inherent to the 10^3 cycles plain fatigue data. Nevertheless, the Dang Van estimation yields significantly less than 10^4 cycles for this case. Compared with the <4000 cycles in the test, this is judged to be a rather good match.

6 Conclusions

In the present investigation, an extensive number of fretting fatigue tests on a specially devised biaxial test rig were carried out for Ti64 and IN718 in self-contact with flat rounded edges contact configuration.

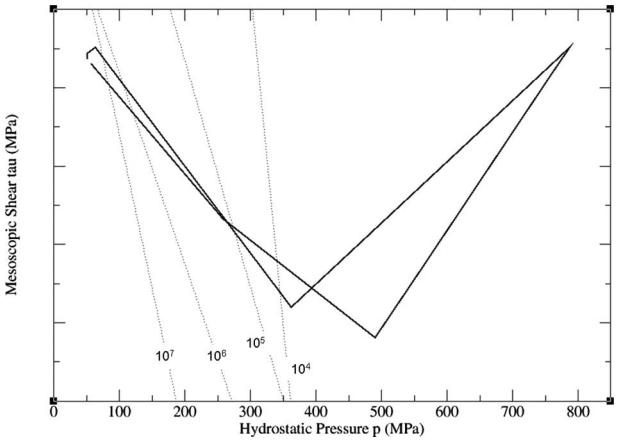

Fig. 17 Averaged Dang Van loading path (REV) for critical location on blade contact surface

1. All tests conditions were reproduced with a two-dimensional plane strain finite element model, and the corresponding stress and strain conditions were calculated until a stabilized material response was reached.
2. From the friction coefficient measurements of the rig, a nonlinear friction model was developed and calibrated against the measured force-displacement loops using the finite element model of the rig assembly.
3. Based on the test rig results, the predictive accuracy of several multiaxial stress based lifing models was tested. The Dang Van life model has proven to yield the most accurate results.
4. The Dang Van method was extended from a pass-no-pass criterion to a quantitative method by introducing an interpolation technique between the lines of constant life.
5. Due to the high stress gradients occurring at the edges of contact, evaluating the Dang Van criterion, solely on the most critical node, has proven to yield too conservative results
6. To overcome the conservative tendency, the so called REV technique was employed. This technique averages the mesoscopic Dang Van loading paths within a certain volume at each time instant.

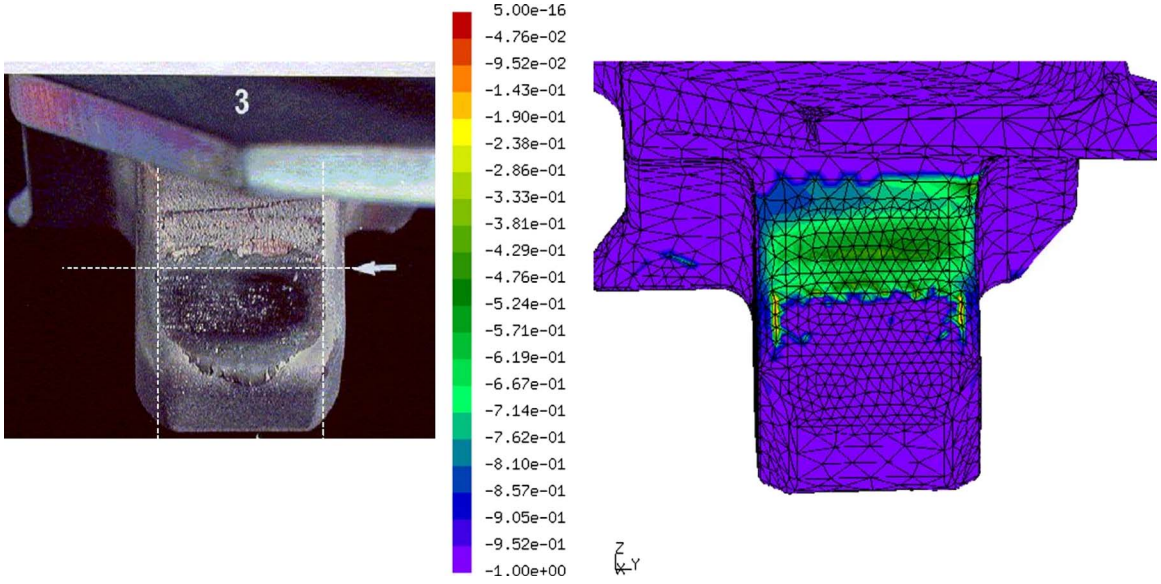

Fig. 16 Damage location as observed in engine tests compared with Dang Van damage distribution from FEA

7. The size of the REV was calibrated by evaluating the Dang Van criterion on uniaxially loaded notched specimens with different notch factors.
8. Using the REV technique in the life prediction has yielded very good results in predicting the life expectancy of the fretting rig test cases
9. It was shown that the variable friction law can be extended to three-dimensional cases and real industrial applications
10. It was shown that the Dang Van method, together with the REV technique, can be successfully employed to predict life on highly loaded contact surfaces in real turbo machinery applications.

Acknowledgment

The authors gratefully acknowledge the financial support for this project from the German Federal Ministry of Economy in the framework of Lufo3. Furthermore, the authors want to acknowledge the contribution of all the students from École Polytechnique Palaiseau, France and the Royal Institute of Technology from Stockholm, Sweden who performed their master thesis in the framework of this project.

Nomenclature

a, b = material constants of the Dang Van criterion
μ_i = initial friction coefficient
μ_s = stabilized friction coefficient
k = stabilization coefficient of the friction law
δ = accumulated relative slip at each node
$T_{\min}$ = minimum test temperature
$T_{\max}$ = maximum test temperature
$\sigma_{f,\min}$ = minimum test fatigue load
$\sigma_{f,\max}$ = maximum test fatigue load
$p_{\min}$ = minimum test contact pressure
$p_{\max}$ = maximum test contact pressure
$\tau(t)$ = mesoscopic critical plane shear stress
$\sigma_h(t)$ = mesoscopic hydrostatic stress
R_1, R_2 = R-ratios 1 and 2
f_{R1}, f_{R2} = fatigue limits for R-ratios 1 and 2

References

[1] Waterhouse, R. B., 1981, *Fretting Fatigue*, Applied Science, London.
[2] Ruiz, C., and Nowell, D., 2000, "Designing Against Fretting Fatigue in Aero Engines, Fracture Mechanics: Applications and Challenges," *Proceedings of the 13th European Conference on Fracture*.
[3] Johnson, K. L., 1985, *Contact Mechanics*, Cambridge University Press, Cambridge, England.
[4] Hofman, F., Bertolino, G., Constantinescu, A., and Ferjani, M., 2009, "Numerical Exploration of the Dang Van High Cycle Fatigue Criterion: Application to Gradient Effects," J. Mech. Mater. Struct., **4**, pp. 293–307.
[5] Ruiz, C., Boddington, P. H. B., and Chen, K. C., 1984, "An Investigation on Fatigue and Fretting in a Dovetail Joint," Exp. Mech., **24**, pp. 208–217.
[6] Hills, D. A., Nowell, D., and O'Connor, J. J., 1988, "On the Mechanics of Fretting Fatigue," Wear, **125**, pp. 129–156.
[7] Szolwinski, M. P., and Farris, T. N., 1996, "Mechanics of Fretting Fatigue Crack Formation," Wear, **198**, pp. 93–107.
[8] Neu, R. W., Pape, J. A., and Swalla, D. R., 2000, "Methodologies for Linking Nucleation and Propagation Approaches for Predicting Life Under Fretting Fatigue," Fretting Fatigue: Current Technology and Practices, ASTM Paper No. STP1367.
[9] Fouvry, S., Kapsa, P., and Vincent, L., 2000, "A Multiaxial Fatigue Analysis of Fretting Contact Taking Into Account the Size Effect," Fretting Fatigue: Current Technology and Practices, ASTM Paper No. STP1367.
[10] Dang Van, K., Griveau, B., and Message, O., 1982, "On a New Multiaxial Fatigue Limit Criterion: Theory and Application," *Biaxial and Multiaxial Fatigue*, M. W. Brown and K. Miller, eds., EGF, pp. 479–496.
[11] Sines, G., 1959, "Metal Fatigue," *Behaviour of Metals Under Complex Static and Alternating Stresses*, McGraw-Hill, New York.
[12] Petiot, C., Vincent, L., Dang Van, K., Maouche, N., Foulquier, J., and Journet, B., 1995, "An Analysis of Fretting-Fatigue Failure Combined With Numerical Calculations to Predict Crack Nucleation," Wear, **181–183**, pp. 101–111.
[13] Maouche, N., Maitournam, H. M., and Dang Van, K., 1997, "On a New Method of Evaluation of the Inelastic State Due to Moving Contacts," Wear, **203–204**, pp. 139–147.
[14] Van, K. D., and Maitournam, M. H., 2002, "On Some Recent Trends in Modelling of Contact Fatigue and Wear in Rail," Wear, **253**(1–2), pp. 219–227.
[15] Dini, D., and Nowell, D., 2003, "Prediction of the Slip Zone Friction Coefficient in Flat and Rounded Contact," Wear, **254**(3–4), pp. 364–369.
[16] Ciavarella, M., and Demelio, G., 2001, "A Review of Analytical Aspects of Fretting Fatigue, With Extension to Damage Parameters, and Application to Dovetail Joints," Int. J. Solids Struct., **38**(10–13), pp. 1791–1811.
[17] Constantinescu, A., Dang Van, K., and Maitournam, H., 2003, "A Unified Approach of Low and High Cycle Fatigue Based on a Shakedown Concept," Fatigue Fract. Eng. Mater. Struct., **26**, pp. 561–568.
[18] Cheikh, M., Quilici, S., and Cailletaud, G., 2007, "Presentation of KI-COF, A Phenomenological Model of Variable Friction in Fretting Contact," Wear, **262**, pp. 914–924.
[19] Sines, G., 1961, "The Prediction of Fatigue Fracture Under Combined Stresses at Stress Concentrations," Bulletin of the Japan Society of Mechanical Engineers, **4**(15), pp. 443–453.
[20] Sines, G., and Ohgi, G., 1981, "Fatigue Criteria Under Combined Stresses or Strains," ASME J. Eng. Mater. Technol., **103**, pp. 82–90.
[21] Dang Van, K., 1993, "Macro-Micro Approach in High-Cycle Multiaxial Fatigue," *Advances in Multiaxial Fatigue, ASTM STP 1991*, D. L. McDowell and R. Ellis, eds., American Society for Testing and Materials, Philadelphia, PA, pp. 120–130.
[22] Dang Van, K., 1999, "Introduction to Fatigue Analysis in Mechanical Design by the Multiscale Approach," *High-Cycle Metal Fatigue in the Context of Mechanical Design*, K. Dang Van and I. Papadoupoulos, eds., Springer-Verlag, Berlin, pp. 57–88.
[23] Bertolino, G., Constantinescu, A., Ferjani, M., and Treiber, P., 2007, "A Multiscale Discussion of Fatigue and Shakedown for Notched Structures," Theor. Appl. Fract. Mech., **48**(2), pp. 140–151.
[24] Calculix, www.calculix.de